INFRARED THERMOGRAPHY FOR IMPACT DAMAGE ANALYSES ON CURVED CFRP LAMINATES USED IN GEOSTATIONARY SATELLITES

Henrique Coelho Fernandes[a,b], Hans-Georg Herrmann[b,c], Hai Zhang[b,d], Francisco J Goyo Brito[e], Joao Henrique N Dal Pra[e], Jose Ricardo Tarpani[e]

[a] Faculty of Computing, Federal University of Uberlandia,
Uberlandia, 38408-100, Brazil
henrique.fernandes@ufu.br

[b] Fraunhofer IZFP Institute for Nondestructive Testing
Saarbrucken, 66123, Germany
hans-georg.herrmann@izfp.fraunhofer.de

[c] Chair of Lightweight Systems, Saarland University
Saarbrucken, 66123, Germany

[d] Computer Vision and Systems Laboratory, Laval University
Quebec, G1V 0A6, Canada
hai.zhang.1@ulaval.ca

[e] Sao Carlos School of Engineering (EESC-USP)
Sao Carlos, 13.566-590, Brazil
goyo-brito@usp.br; joao.pra@usp.br; jrpan@sc.usp.br

Keywords: carbon fiber-reinforced thermoplastic, impact loading, infrared thermography, curved geometry

Abstract. *Advanced materials such as composite materials are extensively used in military and civil aeronautical industries due to their excellent specific mechanical properties. Techniques and protocols to ensure the quality of parts, components, and structures made with such class of advanced materials, both in the manufacturing stage and throughout its lifetime, are indispensable. Towards this strategy and approach, Non-Destructive Testing and Evaluation (NDT&E) methods play today a fundamental role. Among the most valuable NDT methods for the inspection of composite materials, InfraRed Thermography (IRT) currently holds a prestigious place of prominence. In this paper, IRT was used as NDT tool to assess low-energy ballistically impacted curved CFRP specimens previously submitted to thermal shocks. Advanced image processing techniques were then applied in order to enhance the subtle IRT data sequences. Results were qualitatively compared to ultrasound inspections.*

1. INTRODUCTION

Carbon fiber reinforced composites (CFRP) are widely used in military and civil aeronautical industries due to their excellent specific mechanical properties (i.e., property/density ratio) such as stiffness and strength, relatively high temperature and oxidation resistances [1-3]. Aerospace structural components operating in harsh environments are now built with carbon fiber-reinforced thermoplastic (polyphenylene sulfide – PPS-C) matrix composites (e.g., NASA's Soil Moisture Active Passive - SMAP satellite, https://smap.jpl.nasa.gov/). For laminated composite materials, cyclic stresses followed

by impact loading (caused by mechanical fatigue and/or repeated thermal shocks) gives rise to damages like matrix cracking, interply delamination, fiber/matrix debonding. Therefore, non-destructive testing and evaluation (NDT&E) techniques are essential to ensure structural safety, reliability, and operational life.

Among the most valuable NDT&E methods for the inspection of CFRP, InfraRed Thermography (IRT) currently holds a prestigious place of prominence. Infrared (IR) and thermal methods for NDT&E are based on the principle that heat flow in a material is altered by the presence of some types of anomalies. These changes in heat flow cause localized temperature differences in the material's surface. The imaging or study of such thermal patterns is known as IRT.

In this paper, IRT was used as NDT&E tool [4] to assess low-energy ballistically impacted curved CFRP specimens previously submitted to thermal shocks. Specimens were inspected by means of pulsed thermography in reflection mode, and acquired data was latter processed with advanced signal processing techniques. Results were finally qualitatively compared to ultrasonic testing (UT).

2. MATERIALS AND METHODS

2.1. Inspected samples

Specimens inspected in this work were prepared in order to mimic the conditions found in geostationary satellites. PPS-C Cetex TC1100™ laminated coupons were manufactured in $[0/90]_4$ stacking configuration and subsequently curved (~120 mm) at room temperature. After that, they were subjected to rapid and large temperature-range thermal cycles (i.e., thermal shock condition), by rapidly alternating immersion in, respectively, boiling water and liquid nitrogen with short dwell times to avoid liquid absorption to simulate the most critical thermal condition a geostationary (LEO – Low-Earth-Orbit) satellite can experience. Thermal cycles were applied 0, 150, 300 and 500 times for different specimens. Finally, the coupons were transversely impacted with a cylindrical projectile with 50 J kinetic energy to simulate micrometeoroid impact that can lead to delamination damage to laminate composites. Figure 1 shows an example of an inspected specimen, and Table 1 lists all inspected specimens.

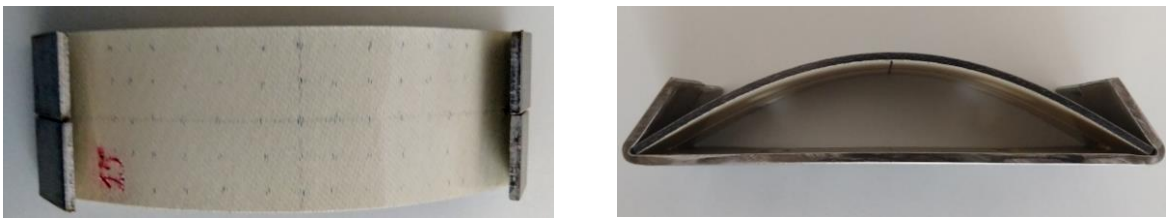

Figure 1 – Frontal (left) and lateral (right) view of a sound specimen for NDT inspection

Table 1 - Characteristics of curved specimens inspected by NDT.

Specimen #	Thermal shock cycles	Impacted (y/n)	Radius of curvature (mm)	Deformation (m/m)	Tension (Pa)	Accumulated energy (J/m^3)
1	150	y	120.30	0.0144	53.493	384.1
2	150	n	121.67	0.0142	52.920	375.9
5	300	y	125.79	0.0138	51.268	352.8
6	300	n	126.61	0.0137	50.951	348.5
12	500	y	115.39	0.0149	55.651	415.7
11	500	n	116.9	0.0148	54.969	405.6
13	0	y	102.46	0.0167	62.252	520.2
15	0	n	118.66	0.0145	54.195	394.2

2.2. Pulsed thermography - PT

In Pulsed Thermography (PT) [5], the specimen is subjected to a heat pulse using a high energy source such as a photographic flash. A heat pulse can be seen as a combination of several periodic waves at different frequencies and amplitudes. After the heat wave comes in contact with the specimen surface, it travels from the surface through the interior of the sample by conduction. As time passes, the specimen surface temperature will drop evenly for a sample without damage or internal defects. Discontinuities on the surface and sub-surface (for example, porosity, delaminations, detachments, broken fibers, inclusions, etc.) can be seen as "barriers" to the heat flow that produce abnormal temperature patterns on the specimen surface, which can be detected with an infrared camera.

Specimens were inspected with a PT set-up in reflection mode. The set-up had an infrared camera (7-14 µm) and a circular flash device with several lamps (3KJ). A short flash was fired for a period of 10µs, and the infrared camera recorded approximately 5s of images at a frame rate of around 145fps. Figure 2 shows the PT setup used in the laboratory for the inspections performed in this work.

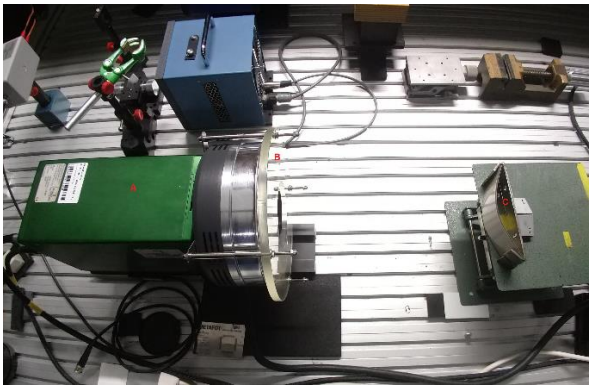

Figure 2 - PT setup (A – IR camera, B – Flash lamps, C – Specimen)

2.3. Principal component thermography - PCT

PT is probably the most investigated IRT method because of its speed (a few seconds for materials with high thermal conductivity to several seconds for materials with low conductivity) and ease of deployment. However, data obtained directly by PT are difficult to analyze. There is a wide variety of processing techniques that have been developed to enhance subtle infrared signatures. One technique that has given good results is called principal component thermography (PCT).

PCT, originally proposed by Rajic (2002) in [6], extracts the image features and reduces the undesirable signals. It relies on Singular Value Decomposition (SVD), which is a tool to extract spatial and temporal data from a matrix in a compact manner by projecting original data onto a system of orthogonal components known as EOF. By sorting the principal components in such a way that the first EOF represents the most characteristic variability of the data, the second EOF contains the second most important variability, and so on, the original data can be adequately represented with only a few EOFs.

The SVD of a MxN matrix A, where $M > N$, can be calculated as follows:

$$A = URV^T \tag{1}$$

where U is a MxN orthogonal matrix, R being a diagonal NxN matrix (with singular values of A present in the diagonal), V^T is the transpose of a NxN orthogonal matrix (characteristic time) as proposed in [5].

Hence, in order to apply the SVD to thermographic data, the 3D thermogram matrix representing time and spatial variations has to be reorganized as a 2D MxN matrix A. This can be done by rearranging the thermograms for every time as columns in A, in such a way that time variations will occur column-wise while spatial variations will occur row-wise. Under this configuration, the columns of U represent a set of orthogonal statistical modes known as EOF that describe the data's spatial variations. On the

other hand, the principal components (PCs), which represent time variations, are arranged row-wise in matrix V^T. The first EOF will represent the most characteristic variability of the data; the second EOF will contain the second most important variability, and so on. Usually, original data can be adequately represented with only a few EOFs. Typically, an IRs sequence of 1000 images can be replaced by 10 or fewer EOFs.

3. RESULTS AND DISCUSSION

Figure 3 shows micrographs of two inspected specimens that were later inspected with IRT. Figure 4 shows the results obtained with PT after PCT processing.

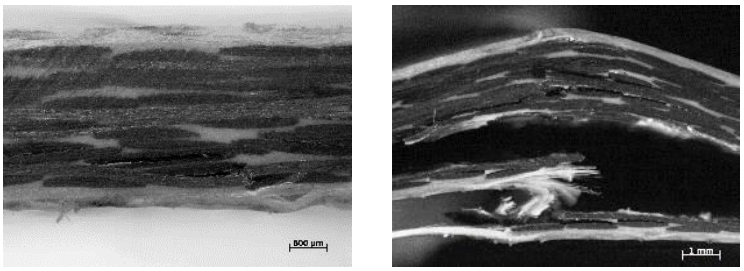

(a) (b)

Figure 3 – Specimens after 500 thermal shock cycles: (a) interply cracking in specimen #11 (not impacted), and (b) catastrophic failure in specimen #12 (impacted).

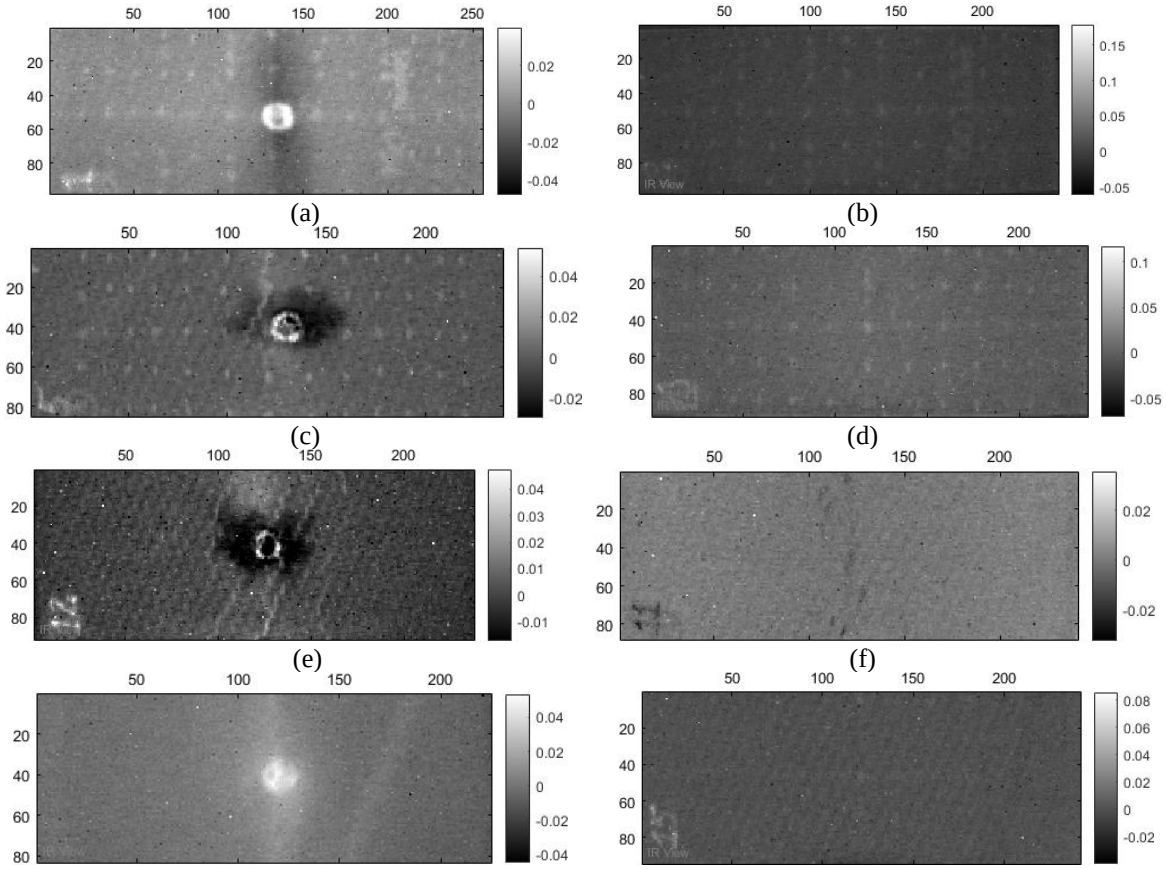

(a) (b) (c) (d) (e) (f) (g) (h)

Figure 4 – Qualitative PCT results: (a) EOF 2 from specimen #1, (b) EOF 2 from specimen #2, (c) EOF 3 from specimen #5, (d) EOF 2 from specimen #6, (e) EOF 3 from specimen #12, (f) EOF 3 from specimen #11, (g) EOF 1 from specimen #13, and (h) EOF 3 from specimen #15.

Figures 4b, 4d, 4f, and 4h show results for two non-impacted curved composite laminates. Figure 4h shows the third EOF obtained by PCT from pristine material condition (i.e., no thermal shocks), while Figure 4f exhibits the third EOF obtained from a specimen previously submitted to 500 thermal shock cycles. One can observe that thermal shocks leaded to small defects (most probably cracks: see the micrographic image shown in Figure 3a) concentrated in the central position of the test specimen. The most of cracks are interfacial (fiber-matrix cracks). However, those can lead to fiber cracks as shown in that figure.

Figures 4a, 4c, 4e, and 4g show results obtained from impacted coupons. Figure 4g corresponds to the specimen without any thermal shock, whereas Figure 4e refers to the specimen previously subjected to 500 thermal shock cycles; note in Figure 3b that the corresponding damage is quite complex and extensive. One can notice that coupon which was not submitted to the thermal shocks (Figure 4g) presents a single crack crossing its entire transverse section. One the other hand, the specimen with 150 thermal shock cycles (Figure 4a) exhibits spread small cracks and delamination; note that these features were intensified as the number of thermal cycles increased, as shown in Figures 4c and 4e, respectively.

This more significant delamination area seen in Figure 4e is probably because of the small cracks the thermal shock cycles caused in the specimen. As observed in Figure 4f and Figure 3a, thermal shocks leaded to minor defects and, these small defects that were already present, lead to a more prominent delamination defect after the cylindrical projectile impact.

Specimens were then submitted to ultrasonic inspection. A 5MHz transducer controlled by a robotic arm was used for inspections. The transducer was moved on the surface of the specimen, and an area of around 38 x 75 mm, with the impact region on the center, was inspected. Figure 5 shows one of these inspections.

Figure 5 - UT inspection

The transducer moved smoothly through the surface of all specimens, except for specimen 13. The impact in this sample caused a sharp edge on the surface of the specimen. Therefore, the transducer had contact problems when passing on the top of specimen 13. This led to a faulty image reconstruction. Figure 6 shows this problem.

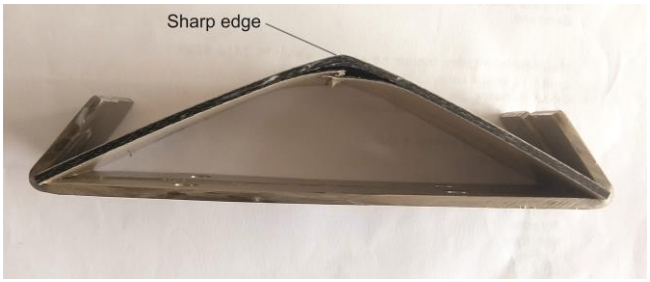

Figure 6 - Specimen 13

Figure 7 and Figure 8 show some results of the UT inspection. All images are 0.9 mm from the surface. One can observe that the inspection of specimen 13 (see Figure 8a) is even smaller in area (37 x 62) due to the sharp edge problem.

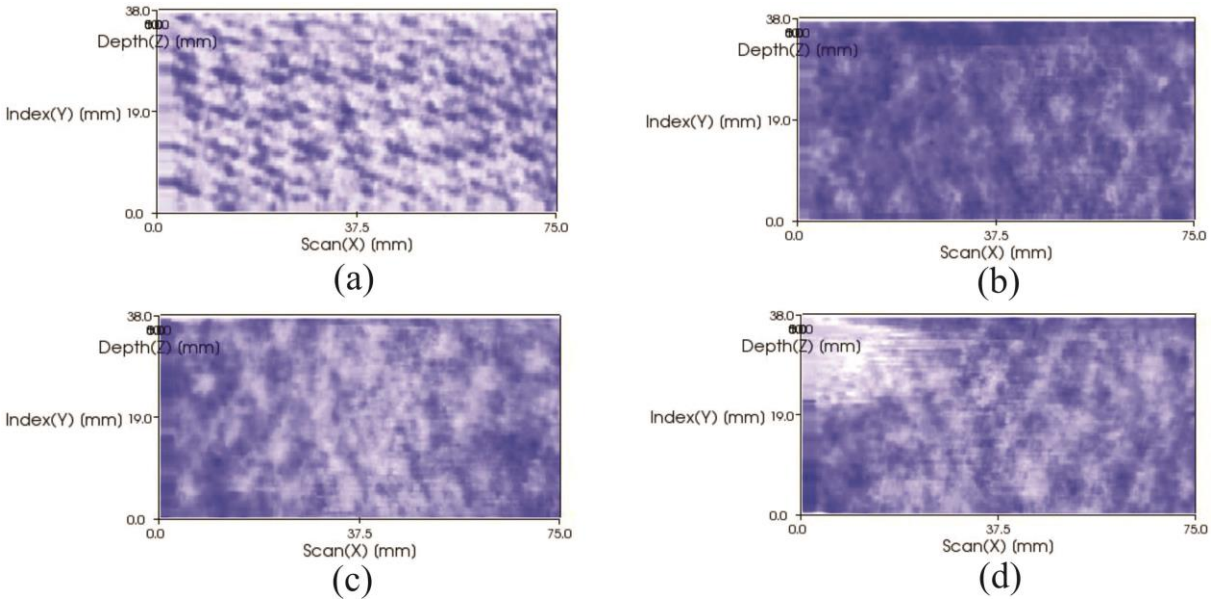

Figure 7 – UT images of 0.9 mm from the surface. Non-impacted specimens: (a) specimen 15, (b) specimen 2, (c) specimen 6, and (d) specimen 11.

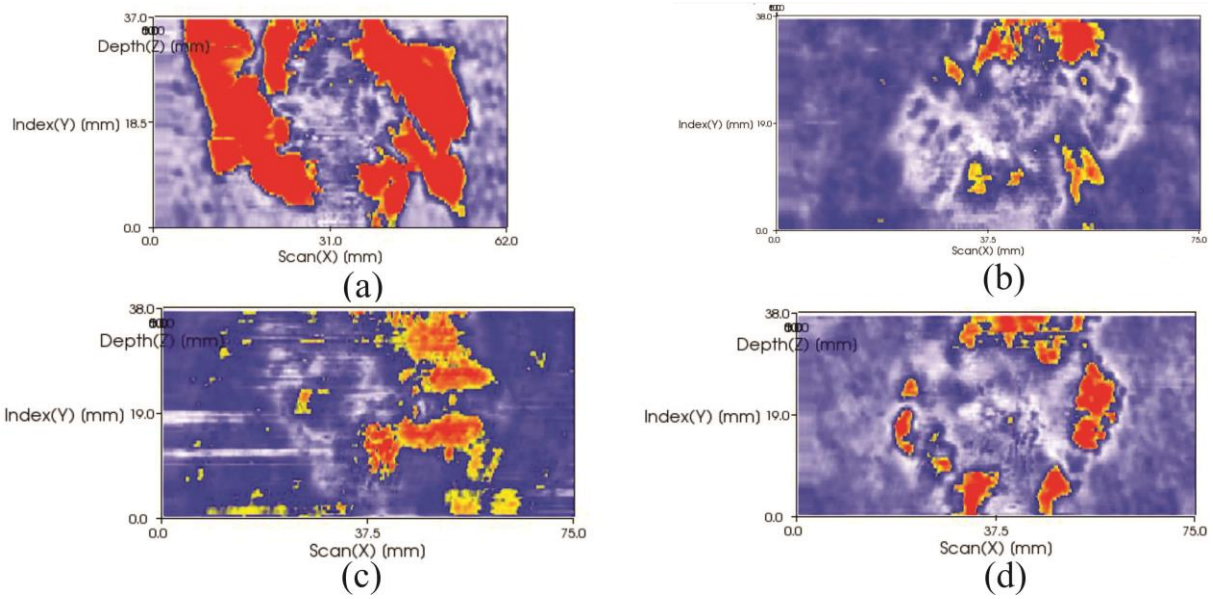

Figure 8 - UT images of 0.9 mm from the surface. Impacted specimens: (a) specimen 13, (b) specimen 1, (c) specimen 5, and (d) specimen 12.

One can see that similarly to the infrared results, UT inspections reveled that specimens with higher thermal shock cycles (Figure 8d – 500 cycles) presented more damage after impacted than specimens with fewer cycles (Figure 8b – 150 cycles).

4. CONCLUSIONS

In this work, specimens prepared in order to mimic the conditions found in geostationary satellites were inspected by infrared thermography and ultrasound. Specimens were curved, submitted to different shock cycles (0, 150, 300, and 500), and then impacted. Results from both NDT&E techniques showed that specimens with higher number of thermal shocks had more damage after the impact.

ACKNOWLEDGEMENTS

This research was funded by the *Coordenação de Aperfeiçoamento de Pessoal de Nível Superior* - Brazil (CAPES) - Finance Code 001, by *Fundação de Amparo à Pesquisa do Estado de Minas Gerais* – Brazil (FAPEMIG) – Finance Code TEC - APQ-01576-18, by the *Alexander von Humboldt Stiftung* – Germany (AvH). The authors express their gratitude to the Brazilian aerospace company Embraer for providing the material tested. JRT is grateful to *Fundação de Amparo à Pesquisa do Estado de São Paulo* – FAPESP (Processes 10/08552-4, 14/25031-9, 15/14702-2, 16/06009-8) for offering him ways to get involved in this study.

REFERENCES

[1] J. Summa, M. Becker, F. Grossmann, M. Pohl, M. Stommel, H.G. Herrmann. *Fracture analysis of a metal to CFRP hybrid with thermoplastic interlayers for interfacial stress relaxation using in situ thermography*. Composite Structures, v.193, p.19–28. (2018).

[2] K. Wang, B. Young, S. T. Smith, *Mechanical properties of pultruded carbon fibre reinforced polymer (CFRP) plates at elevated temperatures.* Engineering structures, v.33(7), p.2154-2161. (2011).

[3] J. Guo, X Gao, E. Toma, et al., *Anisotropy in carbon fiber reinforced polymer (CFRP) and its effect on induction thermography*, NDT & E International, v.91, p.1-8. (2017).

[4] X. Maldague, *Theory and practice of infrared technology for nondestructive testing.* Wiley-Interscience, New York, 1st edition. (2001).

[5] X. Maldague, *Chapter 11 – Techniques of Infrared Thermography: Part 2. Pulse Thermography*. In: Maldague X, Moore P O editors, Nondestructive Handbook, Infrared and Thermal Testing, v.3, p.318–327. The American Society for Nondestructive Testing - ASNT Press, Columbus, OH, 3rd edition. (2001).

[6] N. Rajic, *Principal component thermography for flaw contrast enhancement and flaw depth characterisation in composite structures*. Composite Structures, v.58(4), p.521–528. (2002).

RESPONSIBILITY NOTICE

The authors are the only responsible for the printed material included in this paper.